

Journal of Materials Chemistry B

Accepted Manuscript



This is an *Accepted Manuscript*, which has been through the Royal Society of Chemistry peer review process and has been accepted for publication.

Accepted Manuscripts are published online shortly after acceptance, before technical editing, formatting and proof reading. Using this free service, authors can make their results available to the community, in citable form, before we publish the edited article. We will replace this *Accepted Manuscript* with the edited and formatted *Advance Article* as soon as it is available.

You can find more information about *Accepted Manuscripts* in the [Information for Authors](#).

Please note that technical editing may introduce minor changes to the text and/or graphics, which may alter content. The journal's standard [Terms & Conditions](#) and the [Ethical guidelines](#) still apply. In no event shall the Royal Society of Chemistry be held responsible for any errors or omissions in this *Accepted Manuscript* or any consequences arising from the use of any information it contains.

Cite this: DOI: 10.1039/c0xx00000x

PAPER

www.rsc.org/xxxxxx

Blood activation and compatibility on single-molecular-layer biointerfaces

Shengqiang Nie,^{a,1} Hui Qin,^{a,1} Chong Cheng,^a Weifeng Zhao,^a Shudong Sun,^a Baihai Su,^{b,*} Changsheng Zhao,^{a, c,*} Zhongwei Gu^c

5 Received (in XXX, XXX) Xth XXXXXXXXX 20XX, Accepted Xth XXXXXXXXX 20XX

DOI: 10.1039/b000000x

Research on the interactions between living systems and materials are fuelled by diverse biomedical needs, for example, drug encapsulation and stimulated release, stem cell proliferation and differentiation, cell and tissue cultures, as well as artificial organs. Specific single-molecular-layer biointerface design is one of the most important processes to reveal the interactions or biological responses between synthetic biomaterials and living systems. However, until now, there are limited literatures on comprehensively revealing biomaterials induced blood component activation and hemocompatibility based on the single-molecular-layer interface approach. Thus, in this study, the effects of different groups on blood compatibility are presented using single-molecular-layer silicon (Si) interfaces. Typical hydrophilic groups (hydroxyl, carboxyl, sulfonic, and amino groups) and hydrophobic groups (alkyl, benzene, and fluorinated chains) are introduced onto single-molecular-layer Si interfaces, and confirmed by atomic force microscopy, X-ray photoelectron spectroscopy, and water contact angle. The blood activation and compatibility for the prepared biointerfaces are systematically investigated by protein adsorption, clotting time, Factor XII detection, platelet adhesion, contacting activation, and complement activation experiments. The results indicated that the blood activation and hemocompatibility for the biointerfaces were complex and highly related to the chemical groups and hydrophilicity of the surfaces. Our results further advance the vital importance of carefully designed biointerfaces for specific biomedical applications. The carboxyl group, sulfonic group, and hydroxyl group may be more suitable for interface designs of antifouling materials. Meanwhile, the results revealed that the sulfonic group and fluorinated surface possess great potential for applications of blood contacting devices due to their low contacting blood activation.

1. Introduction

Over the last three decades, research on biomaterials have been fuelled by diverse biomedical needs, such as disposable clinical products, clinical hemodialysis membrane, cardio pulmonary by pass device, and replacement implants, as well as the newly developed drug or antibody nanocarriers. The importance of artificial biomaterials has been recognized and numerous commercialized biomaterials have been brought to market.^{1,2} However, some of these artificial biomaterials are faced with many compatibility problems relating to interaction between artificial materials and tissues during clinical usage, which need to be solved. Foremost among them, are biocompatibility, such as the blood component activation and thrombus generation, cell toxicity, bacterial infection, and inflammation.³⁻⁷ Poor biocompatibility of materials usually result from the unfavorable biointerface or deficiency in surface design. Therefore, the design of advanced biomedical device is highly depended on the

appropriate biochemical interface design to approach favourable biological responses or biocompatibility.⁸⁻¹² The ultimate goal for the surface modification of biomaterials is to confer them with suitable properties for contacting with blood, live tissues and organs both in short-term and long-term applications.¹³⁻¹⁵

However, due to the complexity of the physiology environment, it is difficult to understand the interactions or biological responses between the synthetic biomaterials and living systems. Taking the cellular responses as an example, the chemical composition and physical morphology of biomaterials will affect cell adhesion, migration, proliferation, morphogenesis, polarity, differentiation and apoptosis, as well as tissue development, functionality and regeneration through the complex interactions between cells and a myriad of materials stimuli.^{16,17} In order to conduct and reveal cell-materials interactions, such as cell toxicity, numerous studies have been carried out using well-defined extracellular matrix (ECM).¹⁸⁻²¹ However, the ECM method have been proven to be difficult to use to precisely elucidate how the cells respond to specific biointerface chemical

group.

Over the past decade, the design of single-molecular-layer on silicon or gold interface has been considered to be one of the most important approaches to gain insights into the interactions or biological responses between synthetic biomaterials and living system. Until now, numerous research investigations have been carried out to prepare single-molecular-layer biointerfaces with varied chemical compositions and physical morphologies along different dimensions.²²⁻²⁴ For example, Huang et al. used the patterning of biomolecules on Si substrate for testing the retention of biofunctionalities after surface grafting;²³ Abdul Kafi et al. used nanopillar array for investigating cell adhesion, spreading, and proliferation;²⁵ Wang et al. used plasmonic interface for dynamically monitoring cellular processes;²⁶ Lundgren et al. used Au nanoparticles arrays for controlling cell growth;²⁷ and Padial-Molina et al. designed specific wettability and nanoroughness for investigating cell-materials interactions.²⁸ These studies not only revealed a lot of exciting results on the interactions between living systems and biomaterials, but also guided the applications of biomaterials by integrating the knowledge gained into different advancements.^{24,29-33}

Though, great achievements have been made in relation to these studies, some of the biological interactions caused by biomaterials remain to be explored to the fullest. Among them, blood activation and compatibility are the most important aspects that need to be considered before designed biomaterial is applied to clinical applications. When a biomaterial contacts blood, the interface property will act as the vital factor to govern blood-material interactions. The interface of a biomaterial with poor blood compatibility can result in the adsorption of plasma protein, plasma factors or high molecular weight kininogen; and subsequently promote the transformation of prothrombin into thrombin. Meanwhile, the interface interactions between biomaterials and blood can also induce the activation of platelets and blood coagulation cascade, resulting in thrombi formation. Furthermore, biomaterials also showed activation of complement by alternative pathway; and C3a and C5a are two of the strongest activators of leukocytes and macrophages, which function as the key factors in the complement activation system.

Therefore, diverse research investigations are carried out on the design of blood compatible interface and the exploration of the activation properties of materials, such as hydrophilicity/hydrophobicity, surface charge and distribution, types of surface functional groups, and the length and molecular weight of surface polymer brushes.³⁴⁻³⁶ Some researchers reported that hydrophilic surface could activate the coagulation system and induce thrombin generation, although the surface protein adsorption and platelet adhesion were inhibited by the hydrophilic surface.^{37,38} Other researchers considered that hydrophobic surface could improve the blood compatibility of biomaterials. Latest studies revealed that designing superhydrophobic surface or keeping the balance of hydrophilicity and hydrophobicity at the interface of biomaterials may provide another approach to improve the compatibility issue, for example, the polymeric superhydrophobic surface on carbon nanotube film matrix designed by Sun et al.³⁹ However, these conclusions are based on the complex biointerface system and characteristics such as the intangible length of the polymer

brushes, the difference in the surface charge and distribution, and the difference of the functional groups on the modified material surfaces. Thus, the precise interaction between blood and materials is still not very clear. Until now, there are limited literatures on comprehensively revealing the biomaterials induced blood component activation and hemocompatibility based on the simple silicon or gold interface approach.

In this work, silicon wafer was selected as a substrate on which to detect the detail and to investigate comprehensive blood-material interaction via the approach of single-molecular-layer biointerfaces with different surface hydrophilicity/hydrophobicity. Hydrophilic groups (hydroxyl, carboxyl, sulfonic, and amino groups) and hydrophobic groups (alkyl, benzene, and fluorinated chains) were introduced onto single-molecular-layer Si interfaces. Atom force microscopy (AFM), X-ray photoelectron spectroscopy (XPS), and water contact angle (WCA) were employed to reveal the successful immobilization of the hydrophilic/hydrophobic groups onto the Si surfaces. The blood component activation and compatibility of the prepared single-molecular-layer biointerfaces were investigated by plasma protein adsorption, blood clotting time, Factor XII detection, platelet adhesion amounts and morphologies, contacting activation detection, and complement activation experiments. Finally, we summarized the results on how to facilitate designing biocompatible and functional biointerfaces for specific biomedical or blood contacting applications.

2. Materials and Methods

2.1 Materials

Non-doped silicon wafers <1 1 1>, n-type, were purchased from Hefei Crystal Technical Material Co., Ltd. The silica wafers were polished on both sides, and were sliced into 1 cm × 1 cm before use. 3-glycidioxypropyl trimethoxysilane (GPS, ≥99%), cholamine (≥99%), aminoacetic acid (≥99%), taurine (≥99%), and ethanediamine (≥99%), were purchased from Aladdin (Shanghai, China) and were used without further purification to introduce hydrophilic groups onto the Si surfaces. Butyl amine (≥99%, Aladdin), 2,2,3,3,4,4,4-heptafluorobutylamine (HFM, ≥96%, Sigma Aldrich), and 4-phenylbutylamine (≥98%, Sigma Aldrich), were purchased from Aladdin (Shanghai, China) and were used without further purification to introduce hydrophobic groups onto the Si surfaces. Toluene and chloroform (used as the solvents) were purchased from Chengdu Kelong Inc. (Chengdu, China), and were distilled before use. Bovine serum albumin (BSA) and bovine serum fibrinogen (BFG) were obtained from Sigma Chemical Company. All the other chemicals (analytical grade) were obtained from Chengdu Kelong Inc., and were used without further purification.

2.2. Design of single-molecular-layer biointerfaces on silicon wafer

In this study, silicon wafer was selected as the substrate for three reasons: 1) Si is considered to be a kind of bioinert material; 2) the surface of the silicon wafer is near flat; and 3) silicon surface is easy to be biochemically modified.

2.2.1. Pretreatment of silicon wafer

Prior to silanization, Si wafers were subjected to a clean procedure. The Si wafers were pretreated in acetone, ethanol, and distilled water (immersed for 15 min and sonicated for 2 min for each solution) to remove the impurities on the Si surfaces, respectively. Subsequently, the wafers were processed with "Piranha" solution (a mixture of 70 vol. % concentrated sulphuric acid and 30 vol. % of hydrogen peroxide) at 60 °C for 2 h to remove organic residues. **Caution: "Piranha" solution is an extremely strong oxidant and should be handled and treated with the proper equipment carefully.** Then, the Si wafers were processed in UV/O₃ chamber for 30 min (15 min for each side) to introduce hydroxyl groups on the Si surfaces.

2.2.2. Immobilization of single-molecular-layer GPS on the silicon wafer

After the Si was subjected to UV/O₃, the Si surface was silanized with GPS immediately. According to the literature,⁴⁰ the clean and dry Si substrate was immersed in GPS solution (5 mM, anhydrous toluene as solvent) for 12 h. Then, the GPS immobilized Si (Si-GPS) surface was rinsed and sonicated in pure toluene and dried under nitrogen.

2.2.3. Immobilization of different typical groups on single-molecular-layer biointerfaces

Different hydrophilic group immobilized Si surfaces were obtained via reacting the Si-GPS with cholamine, aminoacetic acid, taurine and ethanediamine, respectively. The Si-GPS was immersed in 125 mM aminoacetic acid (or taurine) aqueous solution at 65 °C for 24 h to obtain carboxyl (or sulfonic) group immobilized Si surface. For the preparation of hydroxyl immobilized Si surface, cholamine was dissolved in anhydrous chloroform to obtain a concentration of 125 mM. After the reflux reaction of Si-GPS with cholamine at 65 °C for 24 h, hydroxyl immobilized Si surface was obtained. To prepare amino group immobilized surface, ethanediamine was firstly single-protected with t-Butyloxy carbonyl (Boc) according to the literature,⁴¹ then dissolved in anhydrous chloroform at a concentration of 125 mM, and reflux reacted with Si-GPS at 65 °C for 24 h. Subsequently, the amino group immobilized Si surface was obtained by the deprotection of Boc using hydrochloric acid. The hydroxyl group, amino group, sulfonic group and carboxyl group immobilized Si wafers were termed Si-OH, Si-NH₂, Si-SO₃H and Si-COOH, respectively.

For the preparation of hydrophobic group immobilized Si surfaces, the Si-GPS was reacted with ethylamine, which was diluted to about 125 mM before use, butyl amine (125 mM, anhydrous chloroform solution), 4-phenylbutylamine (125 mM, anhydrous chloroform solution), and HFM (125 mM, anhydrous chloroform solution) at 65 °C for 24 h, to obtain the alkylated (Si-GPS reacted with ethylamine and butyl amine), phenylated, and fluorinated Si surfaces, respectively; and the obtained hydrophobic group immobilized Si were termed Si-E, Si-B, Si-P and Si-F, respectively.

Additionally, the Si-E, which reacted with ethylamine and exhibited the same basic chain as that of the Si-OH, Si-NH₂, Si-SO₃H and Si-COOH, was used as control sample for performance comparison between the hydrophilic Si surfaces.

2.2.4. Characterization of the immobilized groups

Atom Force Microscopy (AFM) and X-ray photoelectron spectroscopy (XPS)

Before AFM analysis, all the samples were freeze-dried for 6 h to remove the water on the surfaces. AFM images of the samples were acquired using a Multimode Nanoscope V scanning probe microscopy (SPM) system (Bruker, USA). The XPS measurements were performed on an X-ray photoelectron spectroscopy (XSAM800, Kratos Analytical, UK).

Water contact angle (WCA)

The hydrophilicity/hydrophobicity of the Si surface was characterized on the basis of static contact angle measurement using a contact angle goniometer (OCA20, Dataphysics, Germany) equipped with a video capture. For the static contact angle measurement, 3 μL of double distilled water was dropped onto the surface of the sample at room temperature, and the contact angle was measured after 10 s. At least three measurements were averaged to obtain a reliable value. The measurement error was ± 3°.⁴²

2.3. Blood collection

Human blood plasma was used to test the blood compatibility of the samples. Whole human fresh blood was collected by venipuncture from a healthy volunteer (man, 26 years old). The blood was mixed with 3.8 wt. % anticoagulant citrate dextrose (9 : 1, v/v) and centrifuged at 1000 rpm and 4000 rpm for 15 minutes to obtain platelet-rich plasma (PRP) and platelet poor plasma (PPP), respectively.^{15,43} The plasma was stored at -20 °C until use.

2.4. Plasma protein adsorption (BSA and BFG) and platelet adhesion

Protein adsorption experiments were carried out with BSA and BFG solutions. Firstly, the samples (1 × 1 cm²) were immersed in phosphatic buffer solution (PBS), containing BSA and BFG at 1 mg/mL, respectively, and incubated at 37 °C for 1 h; subsequently, the samples were rinsed slightly with PBS solution and double distilled water, respectively. Then, the samples were washed with a solution of (2 wt. % sodium dodecyl sulfate (SDS), 0.05 M NaOH) at 37 °C, and shaken for 2 h to remove the adsorbed protein. More than 95% of the adsorbed protein could be eluted into the SDS solution according to the preliminary experiments. The adsorption and desorption times were carefully determined in the preliminary experiments. The protein concentration was determined using the Micro BCATM Protein Assay Reagent Kit (PIERCE), and then the adsorbed amounts were calculated.⁴⁴

For platelet adhesion, the samples (1 × 1 cm²) were immersed in PBS (pH = 7.4) and equilibrated at 37 °C for 1 h. The PBS was removed, and then 1 mL of fresh PRP was introduced. The samples were incubated with PRP at 37 °C for 30 min. Then the PRP was decanted off, and the samples were rinsed 3 times with PBS. Finally, the samples were treated with 2.5 wt. % glutaraldehyde in PBS at 4 °C for 1 day. The prepared samples were then washed with PBS, and dehydrated by passing through a series of graded alcohol/physiological saline solutions (30%, 50%, 70%, 80%, 90%, 95% and 100 wt. %, respectively, and 15 min for each solution) and isoamyl acetate/alcohol solutions (30%, 50%, 70%, 80%, 90%, 95% and 100 wt. %, respectively, and 15 min for each solution). The critical point drying of the specimens

was done with liquid CO₂. Scanning electron microscopy (SEM) images were recorded using a scanning electron microscope (JSM-5900LV, JEOL, Japan) operated at an accelerating voltage of 20 kV, and the platelet adhesion was investigated. The number of the adhering platelets on the sample surface was calculated from five SEM pictures at 500× magnification from different areas on the same sample.⁴⁴

2.5. Blood clotting time (APTT, PT, and TT) and Factor XII detection

The clotting times including activated partial thromboplastin time (APTT), prothrombin time (PT) and thrombin time (TT), were determined using a semi-automatic blood coagulation analyzer (CA-50, Sysmex, Japan) as follows: the samples (1 × 1 cm²) were placed carefully in a 24-well cell culture plate. Then 250 μL PPP was used to incubate the samples in a well at 37 °C for 0.5 h. Subsequently, 50 μL of the PPP solution was taken for APTT test, and warmed in the automated blood coagulation analyzer for 60 s and then mixed with 50 μL of ACTIN (Siemens Healthcare Diagnostics Products GmbH) agent at 37 °C for 3 minutes, and followed by adding calcium chloride solution (0.025 M, Dade Behring Marburg GmbH). For PT test, 100 μL of the PPP solution was warmed in the automated blood coagulation analyzer for 60 s and then mixed with 100 μL of Thromborel[®] S (Dade Behring Marburg GmbH) agent at 37 °C for 3 minutes.⁴⁵ For TT test, 100 μL of the PPP was incubated in a test cup at 37 °C for 2 min, followed by adding 50 μL of thrombin agent (incubated 10 min at 37 °C before use, Sysmex). The clotting times for APTT, PT and TT were automatically collected and printed by the equipment. The assays were performed in triplicate for each sample.¹²

In this study, the semi-automated blood coagulation analyzer CA-50 (Sysmex Corporation, Kobe, Japan) was employed to detect the Factor XII. The purpose of detecting Factor XIIa was to determine whether the Factor XII was adsorbed or reacted with the Si surface when in contact with the plasma, and to determine whether it resulted in prolonged APTT. The test method was described as follows: The samples were immersed in 200 μL PBS (pH = 7.4) at 4 °C for 24 h, and then at 37 °C for 1 h before use. Subsequently, the PBS was removed and 100 μL of PPP was introduced. After incubating at 37 °C for 30 min, 5 μL of the PPP was added into a test cup, and a mixture of Owren's Veronal Buffer (45 μL) and Factor XII-deficient plasma (50 μL, Sysmex) was added simultaneously. The procedure followed was the same as that of the APTT test. Three independent experiments were conducted to obtain a reliable value.⁴⁶

2.6. Contact activation of coagulation system (thrombin generation and platelet activation)

Commercial enzyme-linked immunosorbent assays (ELISA) were used to evaluate the coagulation activation (thrombin-antithrombin III complex (TAT), Enzygnost TAT micro (Assay Pro, USA) and platelet activation (Platelet Factor 4 (PF-4), CUSABIO BIOTECH CO., LTD, China). The samples were incubated with whole blood for 2 h, and centrifuged for 15 minutes at 1000 g (4 °C) centrifugal force to obtain plasma. Then, these detections were carried out according to the respective instruction manuals.

2.7. Complement activation in human blood system

The same as the PF-4 and TAT tests, the complement activation (C3a and C5a) evaluation of the samples was also carried out with ELISA method (CUSABIO BIOTECH CO., LTD, China). The whole blood in which the samples were incubated for 2 h was centrifuged for 15 minutes at 1000 g (4 °C) centrifugal force to obtain plasma. Then, the TAT and PF-4 detections were carried out according to the respective instruction manuals.

3. Results and Discussion

3.1. Preparation of single-molecular-layer biointerface on silicon wafer

Silicon wafers were selected as the substrate to detect the detail and comprehensive blood-material interaction via the approach of single-molecular-layer biointerfaces with different surface hydrophilicity/hydrophobicity. In this study, typical hydrophilic groups (hydroxyl, carboxyl, sulfonic, and amino groups) and hydrophobic groups (alkyl, benzene, and fluorinated chains) were introduced onto single-molecular-layer Si interfaces. For hydrophilic group immobilized Si surfaces, hydroxyl, carboxyl, sulfonic group and amino group are selected, since these hydrophilic groups are typically found both in natural biopolymers and synthesized polymers, such as protein, heparin, and poly(vinyl alcohol). Alkyl, benzene, and fluorinate groups are the typical hydrophobic polymer components, found in synthetic polymers such as polyethylene and polytetrafluoroethylene; these were selected to prepare the hydrophobic immobilized Si surfaces.

Figure 1 (A) shows the procedure for the preparation of hydrophilic and hydrophobic group immobilized Si surfaces. As shown in the figure, the preparation process involved three steps: 1) pretreatment of Si; 2) silanization of Si by GPS; and 3) immobilizing hydrophilic or hydrophobic groups onto Si surfaces. In the first step, organic residues were removed by "Piranha" solution, and the hydrophilicity of the Si surface was improved (water contact angle: 25 ± 3°), since the "Piranha" solution could introduce hydroxyl group on the Si surface. More hydroxyl groups were introduced after the treatment with UV/O₃ (water contact angle: 8 ± 2°),⁴⁷ and then the silanization reaction could be easily carried out. Elemental analysis of the Si surface was detected by XPS before and after UV/O₃ treatment, see Supporting Information (Table 1S). The results showed that the content of O increased after treating with UV/O₃. Immobilization of hydrophilic/hydrophobic groups on the Si surfaces was achieved via the coupling reaction between the epoxy group and the amino group under mild experimental conditions. In addition, the reactivity between the epoxy group and amino group was the highest compared with those of the epoxy group and carboxyl and hydroxyl groups. For the preparation of Si-NH₂, the reagent diethylamine was single-protected by Boc to avoid the reaction of the two amino groups in diethylamine with the epoxy groups.

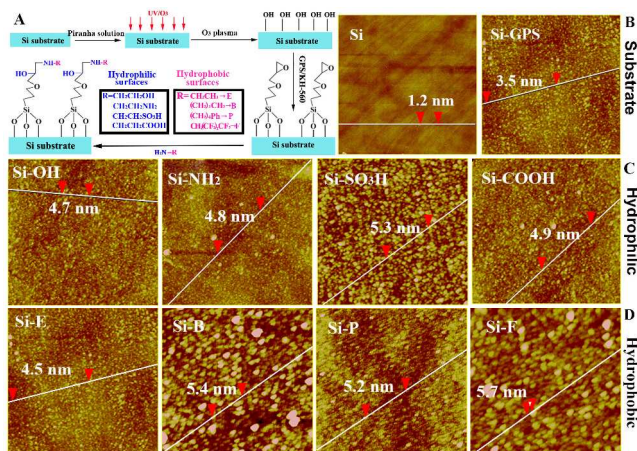


Figure 1 (A) Synthetic procedure for the hydrophilic/hydrophobic group immobilized Si surfaces. (B)-(D) AFM images for Si substrate, hydrophilic and hydrophobic group immobilized Si surfaces (the scan area of each sample was $2.5 \times 2.5 \mu\text{m}^2$).

3.2. Characterization of single-molecular-layer biointerface

In order to determine the morphology of the Si surfaces before and after immobilizing the hydrophilic/hydrophobic groups, atomic force microscopy (AFM) was carried out. Figure 1 (B)-(D) shows the morphology of the Si substrate, hydrophilic, and hydrophobic group immobilized Si surfaces detected by AFM. The surface morphology of Si surface was flat before treating with GPS. Interestingly, the surface of Si-GPS was rougher, and the height between the high spot and low spot was approximately 3.5 nm. While, as shown in Figure 1 (C), the heights for the Si-OH, Si-COOH, Si-SO₃H and Si-NH₂ were approximately 4.7, 4.9, 5.3 and 4.8 nm, respectively. The Si-GPS surface morphology change after the silanization reaction was attributed to the immobilization of GPS on the Si surface, and the height increase for the hydrophilic group immobilized Si surfaces was attributed to the reaction between the GPS and the amino group. The same phenomenon was found on the hydrophobic group immobilized Si surfaces (Figure 1 (D)).

The elemental compositions of the Si-GPS and the hydrophilic/hydrophobic group immobilized Si surfaces were determined by X-ray photoelectron spectroscopy (XPS), Supporting Information Table 2S. After the reaction with amino groups, the element N appeared on the hydrophilic/hydrophobic group immobilized Si surfaces. Additionally, the elements S and F were found on Si-SO₃H and Si-F surface, respectively. Figure 2 (A) shows the detailed analysis of the narrow-scan XPS C (1s) spectra for the Si surfaces. It was found that the peak at 286 eV which was attributed to the binding energy of -C-N appeared. Furthermore, the characteristic peaks, such as at 288.5 eV of -C=O and at 292 eV of -C-F, were also observed. Compared to the XPS spectrum of the Si-GPS surface (Supporting Information Figure 1S), the binding energy peak of C in epoxy group was 287 eV; however, after reacting with amino group, the peak disappeared, and a new peak at 286.2 eV appeared. It revealed that the epoxy groups were successfully reacted with the amino groups. Additionally, the grafting molar ratios of each group were calculated from XPS results, and the data are shown in Supporting Information. By comparing the grafting molar ratios of the groups, it could be found that the grafting molar ratios

were at the same level.

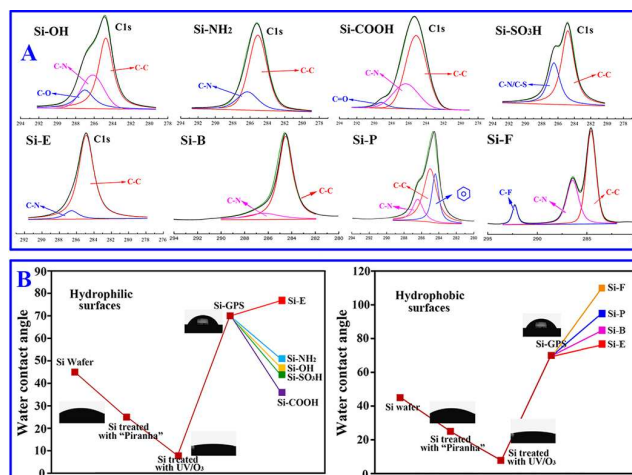


Figure 2 (A) Narrow-scan XPS C (1s) spectra for hydrophilic and hydrophobic group immobilized Si surfaces. (B) Water contact angles for hydrophilic and hydrophobic group immobilized Si surfaces; the values are the average data from 3 samples and the measurement errors for the samples are within 3°.

Water contact angle (WCA) is a convenient way to assess the hydrophilicity/hydrophobicity of a material surface.⁴⁸ Figure 2 (B) shows the WCAs for the hydrophilic/hydrophobic group immobilized Si surfaces. After treating with UV/O₃, the WCA of the Si surface decreased to 8°. However, the WCA for the Si-GPS surface increased to 70°, which indicated that the epoxy group enriched on the Si-GPS surface. After immobilizing the hydrophilic groups, the WCA decreased. The WCA for the Si-COOH was the lowest (36°). On the other hand, the WCAs for the Si-F, Si-P and Si-B increased compared to that for the Si-GPS, and the WCA for the Si-F was the highest (110°). Moreover, for the hydrophobic Si-E surface, the WCA slightly increased (77°) since the -CH₃ was enriched on the Si-E surface. From the results of AFM, XPS and WCA, it was concluded that the hydrophilic/hydrophobic groups were successfully immobilized onto the Si surfaces.

3.3. Protein adsorption and platelet adhesion

Protein adsorption is considered to be the first step when a material surface contacts with blood.⁴⁹ The adsorbed protein on the material surface may activate the Factor XII to Factor XIIa; simultaneously, activate high molecular weight kininogen and prekallikrein. Then, the Factor XIIa converts the prekallikrein into kallikrein and activates Factor XI to Factor XIa, with the high molecular weight kininogen as the cofactor.⁵⁰ Finally the Factor XIa activates the intrinsic pathway of coagulation cascade, and promotes the conversion of fibrinogen into fibrin, and then formation of thrombus. Therefore, protein adsorption is an important way to evaluate the blood compatibility of materials.^{51,52}

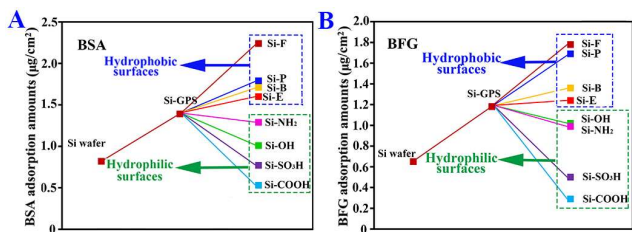


Figure 3 Protein adsorption amounts on the hydrophilic/hydrophobic group immobilized Si surfaces. (A) is for the bovine serum albumin adsorption amounts; and (B) is for the bovine serum fibrinogen adsorption amounts. Note, the values are the average data from 5 samples and the measurement errors for the samples are within $0.05 \mu\text{g}/\text{cm}^2$.

BSA and BFG are chosen as representative plasma proteins to carry out protein adsorption tests, since albumin is the most abundant protein in plasma, while fibrinogen plays an important role in coagulation cascade. Figure 3 shows the amounts of BSA and BFG adsorbed on the hydrophilic/hydrophobic group immobilized Si surfaces. Both for BSA and BFG, after immobilizing the hydrophilic groups on the Si surfaces, the quantity of protein adsorbed decreased compared with Si-GPS and Si-E samples. The lowest amount of protein adsorbed was found on the Si-COOH surface. On the contrary, after immobilizing the hydrophobic groups on the Si surfaces, the quantity of protein (BSA or BFG) adsorbed increased compared with those on the Si-GPS and Si-E surfaces, and the highest protein adsorbed was found on the Si-F surface. Interestingly, it was found that the results of protein adsorption were consistent with those of the WCAs. It was concluded that the hydrophilic/hydrophobic properties of the Si surfaces played an important role in protein adsorption. In recent years, some researchers reported that the water of contacting phase played an important role when a material surface contacted with blood.⁵³ The water of contacting phase could be divided into free-water and combined-water. When the material surface contacted with blood, the high hydrophilic surface could preferentially combine with water and form combined-water enriched surface which inhibited further adsorption of protein with resultant low protein adsorption.

During the past decades, many studies revealed that the protein adsorption results obtained in vitro were quite different from those obtained in vivo, since the interaction between the contacting materials and human blood are more complicated in the in vivo environment. In this study, we used single-molecular-layer biointerfaces, which have not been reported in other studies, to systematically investigate blood compatibility, such as blood coagulation system, blood components activation, platelets adhesion, complement activation, etc. The in vitro investigation of the interaction between single-molecular-layer biointerfaces and blood could eliminate multiple interferences in the complex human blood in vivo environment, and help us clearly comprehend the interactions between functional groups and blood components. It should be stated though that the results obtained from these types of in vitro experiments will be quite different compared with those obtained from in vivo investigations.

For blood-contacting materials, platelets adhesion onto the surface of the materials is a key event in thrombus formation. The platelet adhesion is mediated by integrins on the surface of the platelet which bind to adsorbed proteins, especially fibrinogen,

and then induce platelet activation. The activated platelets then accelerate thrombosis as they promote thrombin formation and platelet aggregation.^{54,55} Therefore, platelets adhesion is another important parameter to evaluate blood component activation and hemocompatibility of materials.⁵⁰

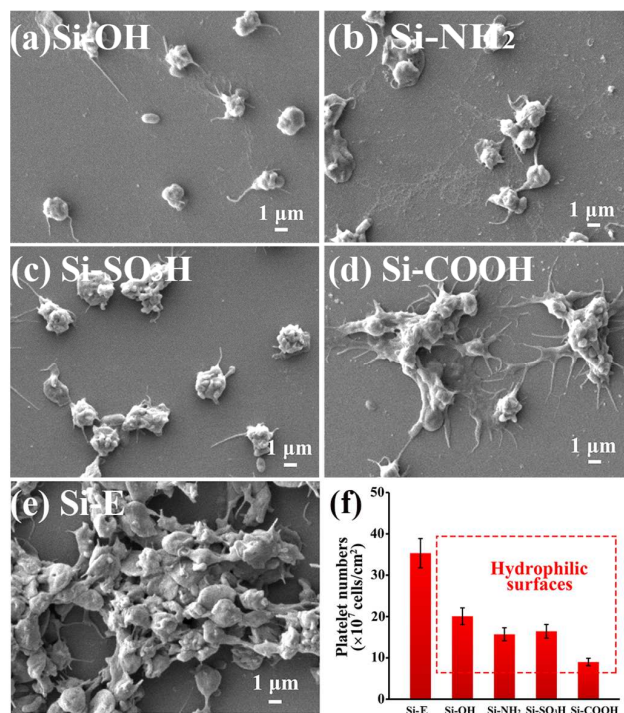


Figure 4 The morphology and amount of platelets adhering on the hydrophilic group immobilized Si surfaces.

Figure 4 and Figure 5 show the adhering platelets amounts and the SEM images of the sample surfaces, respectively. As shown in Figure 4 the adhering platelet amounts on the hydrophilic group immobilized Si surfaces decreased, compared with that on the Si-E surface; and the results were consistent with the WCA and protein adsorption results. Furthermore, it was found that the platelets on the Si-SO₃H, Si-OH and Si-NH₂ surfaces kept nearly original morphologies. However, the morphologies of the platelets on the Si-COOH surface were irregular; numerous platelets were aggregated, and pseudopodium was also found, although the amount of the adhering platelets was the lowest. From Figure 5, it was observed that slight aggregation and deformation of platelets on the Si-F surface occurred, although the amount of the adhering platelets was the highest among the samples. For the Si-B and Si-P surfaces, aggregation and deformation of platelets were also found and pseudopodium was observed. From these results, it could be concluded that the amounts of adhering platelets were related to the surface hydrophilicity, but the morphologies of the adhering platelets were related to the intrinsic properties of the groups rather than the surface hydrophilicity.

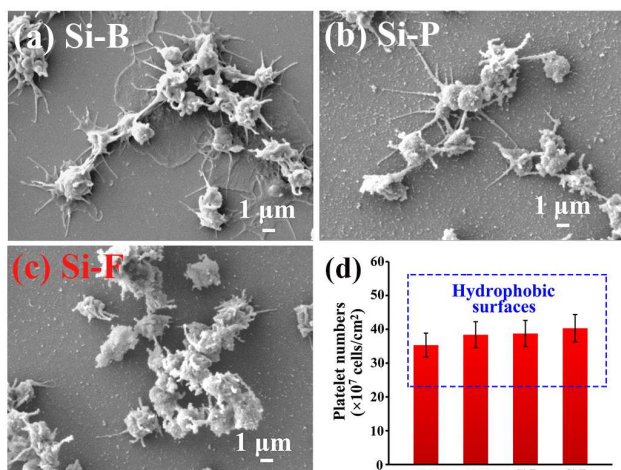


Figure 5 The morphology and amount of platelets adhering on the hydrophobic groups immobilized Si surfaces.

3.4. Clotting time (APTT, PT, and TT) and Factor XII detection

Activated partial thromboplastin time (APTT) and prothrombin time (PT), the global screening procedures used to evaluate coagulation abnormalities in the intrinsic pathway and extrinsic pathway, respectively, can also be used to detect functional deficiencies in factor II, III, V, VIII, X, or fibrinogen.^{56,57} When an anticoagulative material contacts with blood, it might combine or react with the coagulation factors, and the APTT or PT could be prolonged. Thrombin time (TT) is a widely used method to evaluate the anticoagulation ability of blood-compatible materials which is mainly affected by the content and coagulation activity of fibrinogen in plasma. The length of TT reflects the level of fibrinolytic system in common pathway of coagulation cascade.^{58,59}

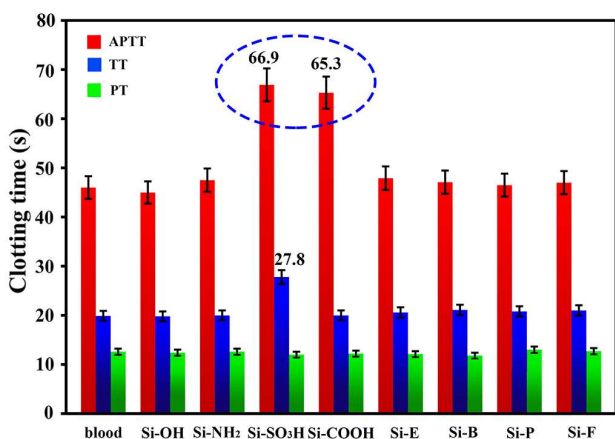


Figure 6 Clotting times (APTT, TT, and PT) for the hydrophilic/hydrophobic group immobilized Si surfaces.

Figure 6 shows the APTT, PT and TT for the hydrophilic/hydrophobic group immobilized Si surfaces. From this figure, it was found that the APTTs for the Si-COOH and Si-SO₃H were prolonged; while the TT was prolonged only for the Si-SO₃H compared with that for Si-GPS. There were no changes with respect to the PTs for all the hydrophilic group immobilized

Si surfaces. For the hydrophobic group immobilized Si surfaces, there is no change in the APTTs, PTs, and TTs compared with that for the Si-GPS. The increment of the APTTs for the Si-COOH and Si-SO₃H might be attributed to the combination or reaction between the functional groups (-COOH and -SO₃H) and the coagulation factors mentioned above; the increase of TT for the Si-SO₃H might be the result from the effect of the -SO₃H group on the fibrinolytic system.

Moreover, Factor XII is considered to be a very important factor in coagulation cascade. When a material contacts with blood, the intrinsic pathway of coagulation cascade may be activated, and the activation of Factor XII is the first crucial step.⁵⁰ Factor XII is activated via absorbing on the material surface, with the effect of the adsorbed protein layer on the material surface. As mentioned above, the activated XII can further promote the activation of Factor XI to XIa, and finally result in thrombus formation. From the data of APTT in Figure 6, the APTTs for the Si-COOH and Si-SO₃H were prolonged. In order to determine whether Factor XII is absorbed or reacted with the functional Si surfaces and then resulted in the deficiency of Factor XII, the APTTs were retested using plasma deficient-XII (in plasma deficient-XII, the Factor XII was eliminated and the other components were the same as in normal plasma).

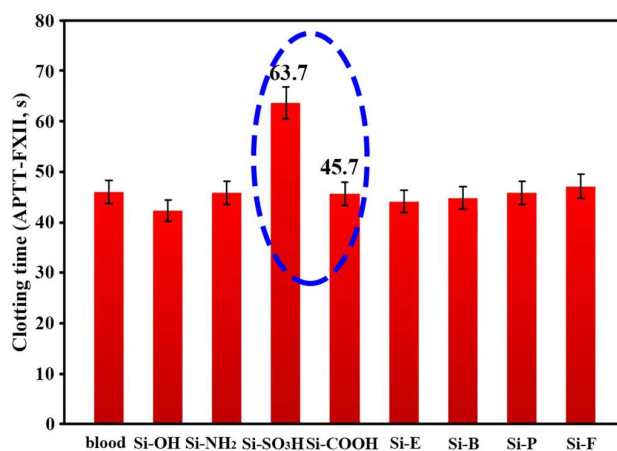


Figure 7 APTTs for the hydrophilic/hydrophobic group immobilized Si surfaces after adding plasma deficient-XII.

Figure 7 shows the APTTs for the hydrophilic/hydrophobic group immobilized Si surfaces after adding plasma deficient-XII (50 μ L) in the tested plasma (5 μ L). As shown in the figure, there was no significant difference in the APTTs for the samples except those for the Si-COOH and Si-SO₃H samples compared with the data in Figure 6. For the Si-COOH sample, the APTT decreased from 65.3 s to 45.7 s, which was the same level as normal plasma. However, for the Si-SO₃H sample, the APTT was slightly decreased, but longer than that of the normal plasma. The results revealed that the prolonged APTT for the sulfonic group immobilized Si surface might be attributed to the deficiency of Factor XII, while the prolonged APTT for the carboxyl group immobilized Si surface had no relationship with the deficiency of Factor XII (likely related to other components in plasma, such as calcium ion mentioned in our previous study⁴⁶).

3.5. Contact activation of coagulation system (platelet activation and thrombin generation)

Contact activation of the coagulation system is considered to be another crucial event when a material contacts with blood. The activated platelets can result in the formation of platelet micro-particles, which can bind and adhere to fibrinogen and fibrin, and then co-aggregate with platelets, even though no adhesion occurs on the material surface; and finally result in thrombus formation and thrombocytopenia in vivo. Furthermore, the activated platelets induce the activation of coagulation cascade which result in thrombin generation and formation of fibrin.⁶⁰⁻⁶² On the other hand, after the contact activation occur, thrombin can be generated by the activation of coagulation cascade. In this study, platelet factor 4 (PF4) was selected to determine the level of platelet activation when blood contacts with the functional Si surfaces, since PF4 was expressed and released after the platelet was activated. Thrombin-antithrombin (TAT) complexes formed following the neutralization of thrombin by antithrombin III have been used as a surrogate marker for thrombin generation.^{63,64} Therefore, the level of thrombin generation in plasma after blood contacted with the functional Si surfaces was also measured.

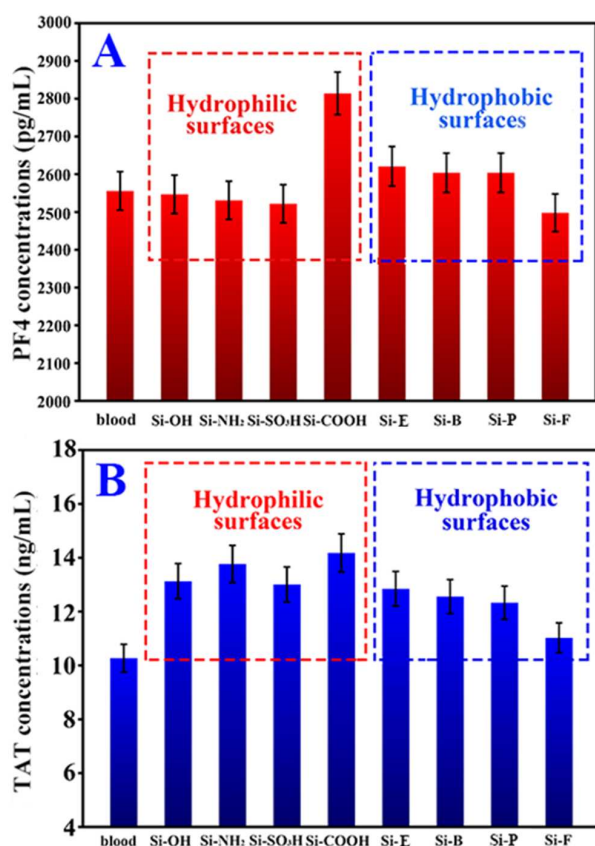


Figure 8 Platelet factor 4 concentrations and thrombin-antithrombin III (TAT) generation for the samples. (A) is for PF4 concentrations; and (B) is for TAT generation level.

Figure 8 shows the PF4 concentrations and TAT levels in plasma after the hydrophilic/hydrophobic group immobilized Si surfaces contacted with blood. From Figure 8 (A), it was observed that for the hydrophilic group immobilized Si surfaces, the PF4 concentration showed slight decrease compared with normal plasma, except for the Si-COOH sample. However, for the hydrophobic group immobilized Si surfaces, the PF4

concentration increased compared with normal plasma. It revealed that the platelet activation occurred after the samples contacted with blood. Compared with the Si-E sample, the PF4 levels for the Si-OH, Si-SO₃H and Si-NH₂ slightly decreased; however, the Si-COOH showed a higher level of PF4. For the hydrophobic group immobilized Si surfaces, the Si-F showed the lowest PF4 among these samples; while the Si-B and Si-P samples showed nearly the same level of PF4 compared with that of the Si-E sample. Compared to the platelets morphologies shown in Figure 5 and Figure 6, it was revealed that the PF4 concentration was related to the platelet morphologies on the Si surfaces. As observed from the TAT level in Figure 8 (B), it was found that the concentrations of the TAT for the Si surfaces increased compared to that for the blood. For the hydrophilic group immobilized Si surfaces, the concentrations were higher than that for the Si-E, especially for the Si-COOH; while for the hydrophobic group immobilized Si surfaces, the concentrations were lower compared with Si-E sample, especially for the Si-F surface. These results revealed that the contact activation of coagulation system may also be affected by other factors such as surface charge and charge density.

3.6. Complement activation

Complement activation is the triggering of the host defense mechanism generated by the localized inflammatory mediator. Thus, it is another vital aspect of blood compatibility. The material surface shows the activation of complement through an alternative pathway. Complement activation could be measured by determining the generated anaphylatoxins C3a, C4a and C5a. In this study, C3a and C5a concentrations were selected for complement activation evaluation using an ELISA assay.

Figure 9 (A) shows the C3a levels for the hydrophilic/hydrophobic group immobilized Si surfaces. As shown in the figure, the C3a concentrations for the Si surfaces increased compared to that for the blood. In addition, the hydrophilic group immobilized Si surfaces showed higher level of C3a concentrations compared with Si-E surface, especially for the Si-COOH and Si-SO₃H surfaces. However, the hydrophobic group immobilized Si surfaces showed lower level of C3a concentrations compared with Si-E, especially the Si-F. The same phenomenon was found in C5a concentration levels (Figure 9 (B)).

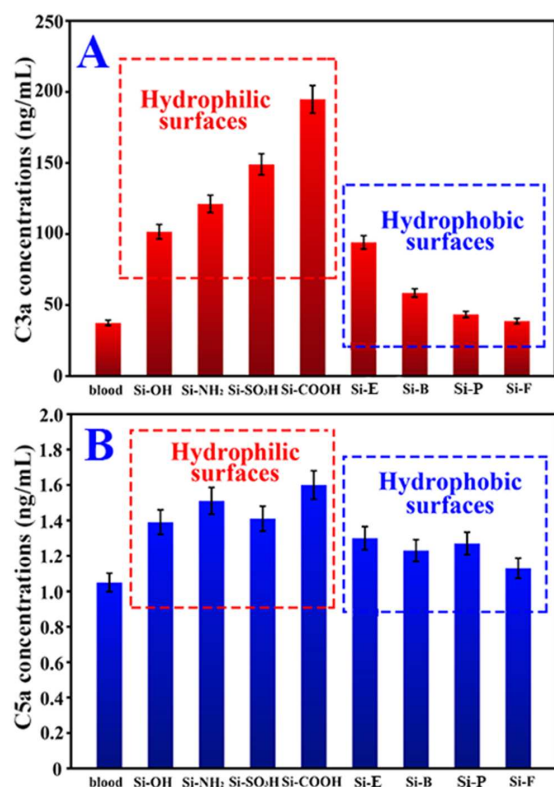
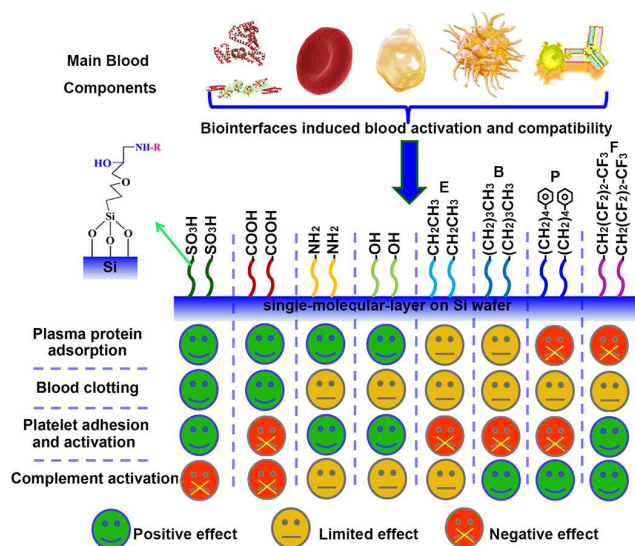


Figure 9 Complement C3a and C5a concentrations after the samples contacted with blood. (A) is for the C3a concentrations; (B) is for the C5a concentrations.

To sum up, this is the first time to comprehensively study the effects of various chemical groups and surface hydrophilicity/hydrophobicity on the blood compatibility and activation by using single-molecular-layer Si interfaces. The conclusive summary of the influences on blood activation and hemocompatibility of the typical chemical groups mentioned in this study is shown in Scheme 1.



Scheme 1 Conclusive summary of influence for typical chemical groups on blood component activation and hemocompatibility based on the single-molecular-layer Si interface approach

According to the results of WCA, protein adsorption and platelet adhesion, the conclusion could be drawn that the anti-protein adsorption and anti-platelet adhesion properties were highly related to the hydrophilicity of the biointerfaces. Hydrophilic surfaces are conducive to decrease the surface protein adsorption and platelet adhesion; while the hydrophobic surfaces present conditions that increase protein adsorption and platelet adhesion. Therefore, the carboxyl, sulfonic, and hydroxyl groups might be more suitable for the design of antifouling material and blood contacting materials. However, it was observed that while the carboxyl group could effectively inhibit protein adsorption and platelet adhesion on its surface, the platelet activation and TAT generation were higher than the other hydrophilic groups. Thus, application of carboxyl group containing polymers on blood contacting or implantable material should be seriously considered, especially the polymers with high carboxyl content, like the poly(acrylic acid). Furthermore, sulfonic groups, with high hydrophilicity, could not only effectively inhibit the protein adsorption and platelet adhesion on biointerface, but also keep the contact activation at a low level; thus, it might present great potential in the applications of blood contacting devices. In this work, interestingly, we found that the fluorinated Si surface could also suppress the platelet activation, TAT generation and platelet morphology deformation, although the protein adsorption and platelet adhesion on its surface were extremely high; these indicated that if the hydrophobic surface design was needed for blood contacting applications, the fluorinated biointerface may be the best choice.

On the other hand, for anticoagulant materials, carboxyl group and sulfonic group are good candidates for the biointerface design, although the anticoagulation mechanisms of these two groups were different. For blood contacting material surfaces in relation to immune system activation, it was found that hydrophobic surface could more effectively inhibit the complement activation compared with hydrophilic surface. Among these groups, the fluorinated Si surface expressed the lowest complement activation; it should be noted that the carboxyl group expressed the highest complement activation. Therefore, fluorinated surface possess the potential to be used in long-term blood contacting device.

4. Conclusion

In order to gain insight into the detailed effects of typical hydrophilic/hydrophobic biointerfaces on blood system, different single-molecular groups were immobilized onto Si surfaces. By systematically investigating plasma protein adsorption, blood clotting time, Factor XII, platelet adhesion amounts and morphologies, contacting activation, and complement activation, we could draw the conclusion that the amounts of protein adsorbed and the amounts of platelets adhering were related to the surface hydrophilicity/hydrophobicity; however, the platelet activation has no direct relation with the surface hydrophilicity/hydrophobicity. The carboxyl group immobilized Si surface showed the highest platelet activation, though the protein adsorption on its surface was the lowest. For clotting times, only the sulfonic group immobilized Si surface could effectively inhibit blood coagulation; and the carboxyl group immobilized Si surface could only effectively prolong the APTT.

On the other hand, for TAT generation and complement activation, the hydrophobic group immobilized Si surfaces showed lower TAT generation and complement activation compared with the hydrophilic group immobilized Si surfaces. Our results may advance the scientific know-how to facilitate designing biocompatible and functional biointerfaces for specific biomedical or blood contacting applications.

Acknowledgments

This work was financially sponsored by the National Natural Science Foundation of China (no. 51173119, and 51225303), and the Program for Changjiang Scholars and Innovative Research Team in the University (IRT1163). We should also thank our laboratory members for their generous help, and gratefully acknowledge the help of Ms H. Wang, of the Analytical and Testing Center at Sichuan University, for the SEM, and Ms Liang, of the Department of Nephrology at West China Hospital, for the fresh human blood collection.

Notes and references

^a College of Polymer Science and Engineering, State Key Laboratory of Polymer Materials Engineering, Sichuan University, Chengdu 610065, People's Republic of China

^b Department of Nephrology, West China Hospital, Sichuan University, Chengdu 610041, People's Republic of China

^c National Engineering Research Center for Biomaterials, Sichuan University, Chengdu 610064, People's Republic of China

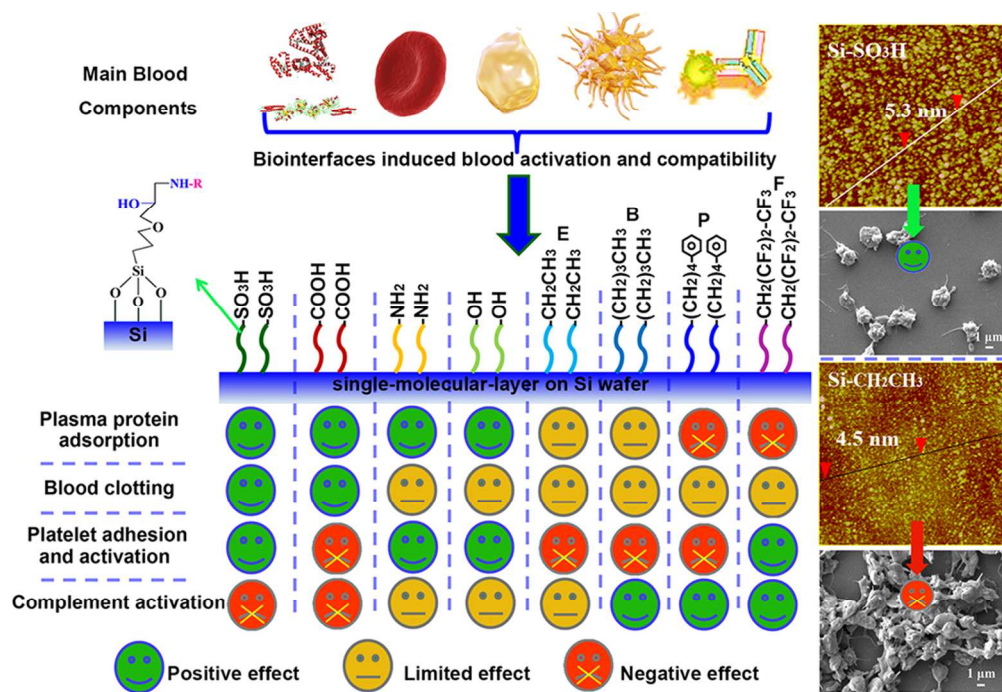
[†] These two authors contribute equally to this work.

*Corresponding author. Tel.: +86-28-85400453; fax: +86-28-85405402. E-mail address: imsbh@163.com (B.H. Su); zhaochsh70@scu.edu.cn or zhaochsh70@163.com (C.S. Zhao).

† Electronic Supplementary Information (ESI) available: [No]. See DOI: 10.1039/b000000x/

- H. Tian, Z. Tang, X. Zhuang, X. Chen and X. Jing, *Prog. Polym. Sci.*, 2012, **37**, 237-80.
- T. T. Ruckh, K. Kumar, M. J. Kipper and K. C. Popat, *Acta Biomater.*, 2010, **6**, 2949-59.
- C. S. Zhao, J. M. Xue, F. Ran and S. D. Sun, *Prog. Mater. Sci.* 2013, **58**, 76-150.
- M. P. Lutolf and J. A. Nat. *Biotech.*, 2005, **23**, 47-55.
- J. J. Rice, M. M. Martino, L. De Laporte, F. Tortelli, P. S. Briquez and J. A. Hubbell, *Adv. Healthc. Mater.*, 2013, **2**, 57-71.
- S. Daghighi, J. Sjollem, H. C. van der Mei, H. J. Busscher and E. T. J. Rochford, *Biomaterials*, 2013, **34**, 8013-7.
- S. H. Lee, M. K. Gupta, J. B. Bang, H. Bae and H. J. Sung, *Adv. Healthc. Mater.*, 2013, **2**, 908-15.
- D. Rana and T. Matsuura, *Chem. Rev.*, 2010, **110**, 2448-71.
- D. Depan and R. D. K. Misra, *Acta Biomater.*, 2013, **9**, 6084-94.
- R. A. Hoshi, R. Van Lith, M. C. Jen, J. B. Allen, K. A. Lapidus and G. Ameer, *Biomaterials*, 2013, **34**, 30-41.
- F. P. Seib, M. Herklotz, K. A. Burke, M. F. Maitz, C. Werner and D. L. Kaplan, *Biomaterials*, 2014, **35**, 83-91.
- C. Cheng, S. Li, S. Q. Nie, W. F. Zhao, H. Yang, S. D. Sun, et al., *Biomacromolecules*, 2012, **13**, 4236-46.
- Y. Kim, D. Rana, T. Matsuura and W. J. Chung, *Chem. Commun.*, 2012, **48**, 693-5.
- R. D. K. Misra, C. Nune, T. C. Pesacreta, M. C. Soman and L. P. Karjalainen, *Acta Biomater.*, 2013, **9**, 6245-58.
- C. Cheng, S. Q. Nie, S. Li, H. Peng, H. Yang, L. Ma, et al., *J. Mater. Chem. B*, 2013, **1**, 265-75.
- H. Shin, S. Jo and A. G. Mikos, *Biomaterials*, 2003, **24**, 4353-64.
- W. Li, P. Zhao, C. Lin, X. Wen, E. Katsanevakis, D. Gero, et al., *Biomacromolecules*, 2013, **14**, 2647-56.
- E. Cukierman, R. Pankov, D. R. Stevens and K. M. Yamada, *Science*, 2001, **294**, 1708-12.
- S. Allazetta, T. C. Hausherr and M. P. Lutolf, *Biomacromolecules*, 2013, **14**, 1122-31.
- S. C. Owen, S. A. Fisher, R. Y. Tam, C. M. Nimmo and M. S. Shoichet, *Langmuir*, 2013, **29**, 7393-400.
- M. Köllmer, V. Keskar, T. G. Hauk, J. M. Collins, B. Russell and R. A. Gemeinhart, *Biomacromolecules*, 2012, **13**, 963-73.
- R. F. Mhanna, J. Vörös and M. Zenobi-Wong, *Biomacromolecules*, 2011, **12**, 609-16.
- M. Huang, B. C. Galarreta, A. Artar, R. Adato, S. Aksu and H. Altug, *Nano. Lett.*, 2012, **12**, 4817-22.
- G. S. Park, H. Kwon, D. W. Kwak, S. Y. Park, M. Kim, J. H. Lee, et al., *Nano. Lett.*, 2012, **12**, 1638-42.
- M. Abdul Kafi, W. A. El-Said, T. H. Kim and J. W. Choi, *Biomaterials*, 2012, **33**, 731-9.
- W. Wang, K. Foley, X. Shan, S. Wang, S. Eaton, V. J. Nagaraj, et al., *Nat. Chem.*, 2011, **3**, 249-55.
- A. Lundgren, Y. Hed, K. Öberg, A. Sellborn, H. Fink, P. Löwenhielm, et al., *Angew. Chem. Int. Edit.*, 2011, **50**, 3450-3.
- M. Padial-Molina, P. Galindo-Moreno, J. E. Fernández-Barbero, F. O'Valle, A. B. Jódar-Reyes, J. L. Ortega-Vinuesa, et al. *Acta Biomater.*, 2011, **7**, 771-8.
- P. Zhang, H. Wu, H. Wu, Z. Lu, C. Deng, Z. Hong, et al., *Biomacromolecules*, 2011, **12**, 2667-80.
- S. Meng, M. Rouabhia and Z. Zhang, *Bioelectromagnetics*, 2013, **34**, 189-99.
- M. Rouabhia, H. Park, S. Meng, H. Derbali and Z. Zhang, *PLoS One*, 2013, **8**, e71660.
- F. Zomer Volpato, J. Almodóvar, K. Erickson, K. C. Popat, C. Migliaresi and M. J. Kipper, *Acta Biomater.*, 2012, **8**, 1551-9.
- D. Depan, T. C. Pesacreta and R. D. K. Misra, *Biomater. Sci.*, 2014, **2**, 264-74.
- C. J. Pan, Y. H. Hou, B. B. Zhang, Y. X. Dong and H. Y. Ding, *J. Mater. Chem. B*, 2014, **2**, 892-902.
- B. C. Dash, G. Réthoré, M. Monaghan, K. Fitzgerald, W. Gallagher and A. Pandit, *Biomaterials*, 2010, **31**, 8188-97.
- M. Wang, J. Yuan, X. Huang, X. Cai, L. Li and J. Shen, *Colloid Surf. B-Biointerfaces*, 2013, **103**, 52-8.
- E. A. Vogler and C. A. Siedlecki, *Biomaterials*, 2009, **30**:1857-69.
- C. Sperling, M. Fischer, M. F. Maitz and C. Werner, *Biomaterials*, 2009, **30**, 4447-56.
- T. Sun, H. Tan, D. Han, Q. Fu and L. Jiang, *Small*, 2005, **1**, 959-63.
- X. Jia, X. Jiang, R. Liu and J. Yin, *ACS Appl. Mater. Interfaces*, 2010, **2**, 1200-5.
- D. Tan, X. Zhang, J. Li, H. Tan and Q. Fu, *Appl. Surf. Sci.*, 2012, **258**, 2697-706.
- L. L. Li, C. Cheng, T. Xiang, M. Tang, W. F. Zhao, S. D. Sun and C. S. Zhao, *J. Membr. Sci.*, 2012, **405-406**, 261-274.
- A. He, B. Lei, C. Cheng, S. Li, L. Ma, S. D. Sun and C. S. Zhao, *RSC Adv.*, 2013, **3**, 22120-9.
- L. Ma, H. Qin, C. Cheng, Y. Xia, C. He, C. X. Nie, et al., *J. Mater. Chem. B*, 2014, **2**, 363-75.
- H. J. Zhou, C. Cheng, H. Qin, L. Ma, C. He, S. Q. Nie, et al., *Polym. Chem.*, 2014. DOI: 10.1039/C4PY00136B.
- S. Q. Nie, M. Tang, C. Cheng, Z. H. Yin, L. R. Wang, S. D. Sun and C. S. Zhao, *Biomater. Sci.*, 2014, **2**, 98-109.
- E. Turan, S. Demirci and T. Caykara, *Thin. Solid. Films*, 2010, **518**, 5950-4.
- T. Nishimura, Boca Raton, FL, CRC, 1993.
- J. Andrade and V. Hlady, *Ann. NY. Acad. Sci.*, 1987, **516**, 158-72.
- M. B. Gorbet and M. V. Sefton, *Biomaterials*, 2004, **25**, 5681-703.
- W. Tsai, J. Grunkemeier, C. McFarland and T. Horbett, *J. Biomed. Mater. Res.*, 2002, **60**, 348-59.
- W. Tsai, Q. Shi, J. Grunkemeier, C. McFarland and T. Horbett, *J. Biomater. Sci. Polym. Ed.*, 2004, **15**, 817-40.
- H. Chen, L. Yuan, W. Song, Z. Wu and D. Li, *Prog. Polym. Sci.*, 2008, **33**, 1059-87.
- J. Grunkemeier, W. Tsai and T. Horbett, *J. Biomater. Sci. Polym. Ed.*, 2001, **12**, 1-20.

-
- 55 J. Grunkemeier, W. Tsai, C. McFarland and T. Horbett, *Biomaterials*, 2000, **21**, 2243-52.
- 56 A. H. Kamal, A. Tefferi and R. K. Pruthi, *Mayo Clinic Proceedings*, Elsevier, 2007. pp. 864-873.
- 57 L. L. Leung, *ASH Education Program Book*, 2006, **2006**, 457-61.
- 58 N. Key, M. Makris, D. O'Shaughnessy and D. Lillicrap, *Practical Hemostasis and Thrombosis: Wiley Online Library*, 2009.
- 59 M. Popović, K. Smiljanić, B. Dobutović, T. Syrovets, T. Simmet and E. R. Isenović, *Mol. Cell Biochem.*, 2012, **359**, 301-13.
- 60 P. Siljander, O. Carpen and R. Lassila, *Blood*, 1996, **87**, 4651-63.
- 61 P. A. Holme, N. O. Solum, F. Brosstad, T. Pedersen and M. Kveine *Thromb. Haemost.*, 1998, **79**, 389-394.
- 62 C. H. Gemmell, *J. Biomed. Mater. Res.*, 1998, **42**, 611-6.
- 63 J. Hong, K. Nilsson Ekdahl, H. Reynolds, R. Larsson and B. Nilsson, *Biomaterials*, 1999, **20**, 603-611.
- 64 R. Blezer, G. M. Willems, P.T. Cahalan and T.Lindhout, *Thromb. Haemost.*, 1998, **79**, 296-301.



88x60mm (300 x 300 DPI)